

## Tissue inhibitor of metalloproteinase-3 inhibits neonatal mouse cardiomyocyte proliferation via EGFR/JNK/SP-1 signaling

Lamis Hammoud,<sup>1</sup> Dylan E. Burger,<sup>1</sup> Xiangru Lu,<sup>3</sup> and Qingping Feng<sup>1,2,3</sup>

Departments of <sup>1</sup>Physiology and Pharmacology and <sup>2</sup>Medicine, University of Western Ontario; and <sup>3</sup>Lawson Health Research Institute, London, Ontario, Canada

Submitted 21 January 2008; accepted in final form 5 February 2009

**Hammoud L, Burger DE, Lu X, Feng Q.** Tissue inhibitor of metalloproteinase-3 inhibits neonatal mouse cardiomyocyte proliferation via EGFR/JNK/SP-1 signaling. *Am J Physiol Cell Physiol* 296: C735–C745, 2009. First published February 11, 2009; doi:10.1152/ajpcell.00246.2008.—We have recently demonstrated that tissue inhibitor of metalloproteinase-3 (TIMP-3) decreases neonatal cardiomyocyte proliferation (Hammoud L, Xiang F, Lu X, Brunner F, Leco K, Feng Q. *Cardiovasc Res* 75: 359–368, 2007). The aim of the present study was to delineate a pathway through which TIMP-3 exerts its antiproliferative effect. Experiments were conducted on neonatal cardiomyocyte cultures and heart tissues isolated from wild-type (WT) and TIMP-3<sup>-/-</sup> mice. Deficiency in TIMP-3 decreased p27 expression and increased cardiomyocyte proliferation in cardiomyocytes and neonatal hearts. A TIMP-3/epidermal growth factor (EGF) receptor (EGFR)/c-Jun NH<sub>2</sub>-terminal kinase (JNK)/SP-1/p27 pathway was investigated. JNK phosphorylation and EGFR protein levels were increased in TIMP-3<sup>-/-</sup> cardiomyocytes and heart tissues. Treatment with recombinant TIMP-3 decreased JNK phosphorylation and EGFR expression/phosphorylation. Inhibition of JNK activity using SP-600125 decreased SP-1 phosphorylation, increased p27 expression, and decreased cardiomyocyte proliferation. Furthermore, treatment with the EGFR specific inhibitor PD-168393 or the EGF-neutralizing antibody decreased cardiomyocyte proliferation as well as phosphorylation of JNK and SP-1 in both WT and TIMP-3<sup>-/-</sup> cardiomyocytes. We conclude that TIMP-3 inhibits neonatal mouse cardiomyocyte proliferation by upregulating p27 expression. The effects of TIMP-3 are mediated via inhibition of EGFR expression/phosphorylation, and decreases in JNK and SP-1 signaling.

epidermal growth factor receptor; signal transduction; c-Jun NH<sub>2</sub>-terminal kinase

EARLY HEART DEVELOPMENT REQUIRES the synchronization of cellular events including proliferation, differentiation, and structural remodeling (21). Fetal and neonatal cardiomyocytes undergo significant levels of proliferation. After a brief period of neonatal proliferation, mammalian cardiomyocytes irreversibly exit the cell cycle. Further growth of the heart occurs only by hypertrophy of the preexisting heart cells (24, 26). In rodents, the cessation of hyperplastic growth occurs ~1 wk after birth (22). Cell cycle inhibitors such as p21 and p27 are crucial in promoting the exit of cardiomyocytes from the cell cycle (6). Indeed, deletion of p27 in mice leads to the continuation of hyperplastic growth in the postnatal heart well beyond the normal cessation point (30). However, although the precise sequence of events involved in the cessation of cardiomyocyte proliferation is believed to be preprogrammed, the mechanism by which it occurs is unknown.

The extracellular matrix (ECM) is crucial for the development and survival of multicellular organisms. The structural and functional integrity of the ECM is ensured through a balance between matrix metalloproteinases (MMPs), which cleave ECM proteins, and their endogenous inhibitors, the tissue inhibitors of metalloproteinases (TIMPs) (37). TIMPs are a family of four homologous proteins, all of which are expressed in the heart (35). Unique among the TIMPs, TIMP-3 inhibits a wide range of MMPs, displays high cardiac expression, and is sequestered to the ECM (38). As it is ECM bound, TIMP-3 may have more influential biological effects compared with the other TIMPs that are soluble and able to diffuse away from the interaction site. A number of studies have established an important physiological role for TIMP-3 within the heart, because its absence leads to myocardial dysfunction (13, 14). Furthermore, TIMP-3 also regulates neonatal cardiomyocyte proliferation. In this regard, we recently demonstrated that neonatal cardiomyocyte proliferation was increased in TIMP-3<sup>-/-</sup> cardiomyocytes, whereas treatment with recombinant TIMP-3 (rTIMP-3) inhibited proliferation (17). However, the mechanism through which TIMP-3 exerts its antiproliferative effect on cardiomyocytes remains unknown.

Epidermal growth factor (EGF) receptor (EGFR), a receptor tyrosine kinase that belongs to the family of ErbB receptors, has been implicated in promoting proliferation in many cell types including vascular smooth muscle cells (23) and fetal cardiomyocytes (16, 41). The ligands of EGFR consist of a family of structurally and functionally related integral membrane proteins that can be proteolytically cleaved and shed from cells (18, 32). EGFR ligands include EGF, transforming growth factor- $\alpha$ , heparin-binding EGF-like growth factor, betacellulin, amphiregulin, epiregulin, and epigen (32). The binding of ligands to EGFR leads to activation of mitogen-activated protein kinases (MAPKs) including c-Jun NH<sub>2</sub>-terminal kinase (JNK), p38, and extracellular signal-related kinase (ERK) in several cell types (4, 10, 33). Interestingly, metalloproteinase activity is critical for EGFR ligand shedding (32). TIMP-3, through its inhibition of metalloproteinases, has been shown to inhibit EGFR signaling in cancer cells (1, 11). However, the effect of TIMP-3 on EGFR regulation in cardiomyocytes has not been investigated.

The aim of the present study was to elucidate the signaling pathway by which TIMP-3 inhibits proliferation in mouse neonatal cardiomyocytes. We hypothesized that TIMP-3 inhibits cardiomyocyte proliferation by increasing the levels of cell cycle inhibitors present within the cardiomyocytes via inhibi-

Address for reprint requests and other correspondence: Q. Feng, Dept. of Physiology & Pharmacology, Univ. of Western Ontario, London, Ontario, Canada N6A 5C1 (e-mail: qfeng@uwo.ca).

The costs of publication of this article were defrayed in part by the payment of page charges. The article must therefore be hereby marked "advertisement" in accordance with 18 U.S.C. Section 1734 solely to indicate this fact.

tion of EGFR signaling, and downstream MAPK signaling. To test these hypotheses, a primary cell culture model of neonatal mouse cardiomyocytes obtained from wild-type (WT) and TIMP-3<sup>-/-</sup> mice was employed. Changes in cell proliferation were further confirmed *in vivo*. Expression of EGFR and p27 and phosphorylation of MAPK and SP-1 were assessed. Our study suggests that TIMP-3 inhibits neonatal cardiomyocyte proliferation by downregulation of EGFR/JNK signaling pathway.

## MATERIALS AND METHODS

**Animals.** WT mice of the genetic background C57BL/6 were obtained from Jackson Laboratories (Bar Harbor, ME). TIMP-3<sup>-/-</sup> mice were generated as described previously (20). A breeding program was carried out to generate neonates for this study. Animal studies were approved by the University of Western Ontario Institutional Animal Care and Use Committee, and the investigation conformed with the *Guide for the Care and Use of Laboratory Animals*, published by National Institutes of Health (NIH Publication No. 85-23, Revised 1996).

**Isolation and culturing of neonatal mouse cardiomyocytes.** The neonatal cardiomyocyte cultures were prepared from mice born within 24 h as in our previous reports (7, 21, 28, 34). Noncardiomyocytes were removed through 1 h of preplating, after which cardiomyocytes were plated in M199 medium containing 10% fetal bovine serum (FBS) on culture plates precoated with 1% gelatin (Sigma). Neonatal cardiomyocytes were incubated at 37°C and 5% CO<sub>2</sub> in a humidified chamber. A subconfluent spontaneously beating monolayer of cardiomyocytes was formed within 2 days (7, 21).

**Purity of cardiomyocyte culture.** Cardiomyocytes were seeded on coverglasses precoated with 1% gelatin and cultured to subconfluence for 72 h. Cells were fixed in 20% acetone-80% methanol for 30 min at 4°C, washed with PBS, and incubated overnight at 4°C with a mouse monoclonal antibody to sarcomeric  $\alpha$ -actinin (1:500; Sigma). Subsequently, cells were incubated with a fluorescent anti-mouse secondary antibody (1:500; Jackson ImmunoResearch Lab) for 1 h. Nuclei were stained with Hoechst 33342 (1  $\mu$ g/ml), and slides were then mounted and visualized using a Zeiss Observer D1 microscope. Cardiomyocytes were identified by sarcomeric  $\alpha$ -actinin staining.

Purity was also verified through flow cytometry. Cells were cultured to subconfluence for 72 h, permeabilized using Foxp3 Staining Buffer Set (eBioscience) as per manufacturer's instructions, and subsequently stained with a mouse monoclonal antibody to cardiac-specific  $\alpha$ -actinin (1:250; Sigma) for 30 min. Cells were then incubated with an FITC-conjugated anti-mouse secondary antibody (1:500; Jackson ImmunoResearch Lab). Samples were analyzed using flow cytometry.

**Cellular proliferation.** To determine the effect of TIMP-3, JNK, SP-1, and EGFR on cardiomyocyte proliferation, neonatal cardiomyocytes isolated from WT and TIMP-3<sup>-/-</sup> mice were cultured as described above and seeded at a cell density of 100,000 cells/well in 96-well plates precoated with 1% gelatin. Eighteen hours following cell seeding, cardiomyocytes were treated with 1  $\mu$ g/ml recombinant

mouse TIMP-3 (rTIMP-3, EMD Biosciences) or 10  $\mu$ M selective JNK inhibitor (SP-600125, Sigma), 10  $\mu$ M EGFR inhibitor (PD-168393, EMD Biosciences), 10 nM SP-1 inhibitor mithramycin (MMA; Sigma), 20  $\mu$ g/ml EGF neutralizing antibody (Upstate Biotechnology), or 100 ng/ml recombinant EGF (rEGF; R&D Applied Biosystems) in M199-10% FBS and cultured for another 54 h. Although all above pharmacological inhibitors are selective, some nonspecific effects may not be completely excluded. For measurements of EGFR phosphorylation, cells were incubated with rEGF for 10 min. Cellular proliferation was assessed at 72 h postseeding by cell counts using a hemocytometer by two independent investigators, cell proliferation assay kit, and bromodeoxyuridine (BrdU) staining.

A CyQuant cell proliferation assay kit (Molecular Probes) was used to measure cell proliferation as per manufacturer's recommendation. Fluorescence was measured using a SpectraMax M5 microplate reader (Molecular Devices) using excitation and emission wavelengths of 480 and 520 nm, respectively. A standard curve was created to convert sample fluorescence values into cell numbers.

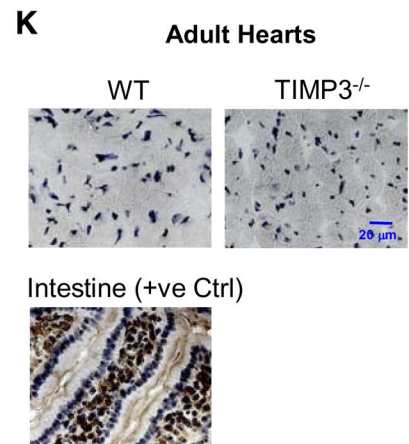
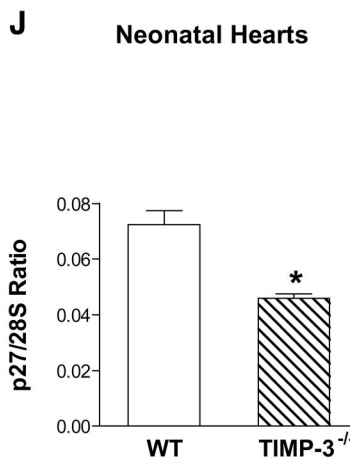
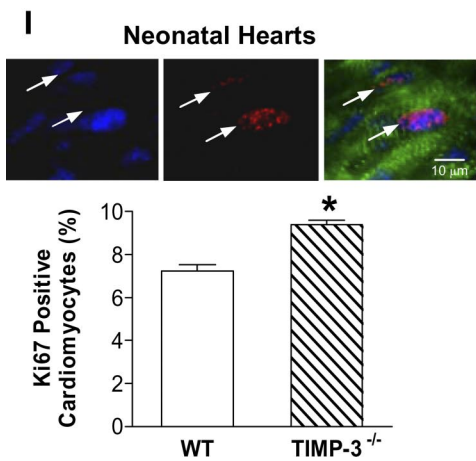
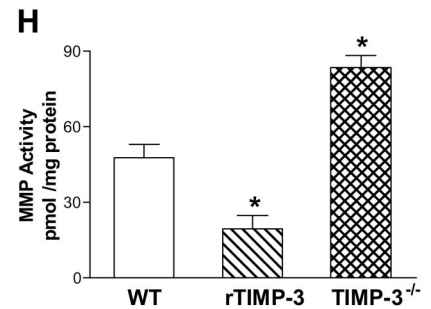
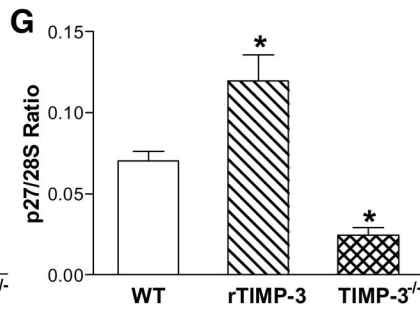
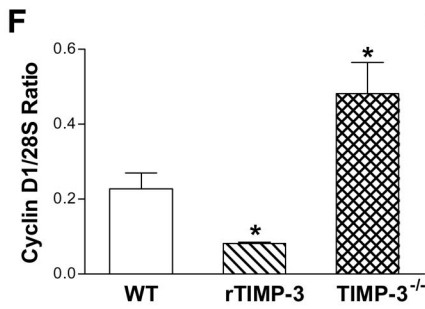
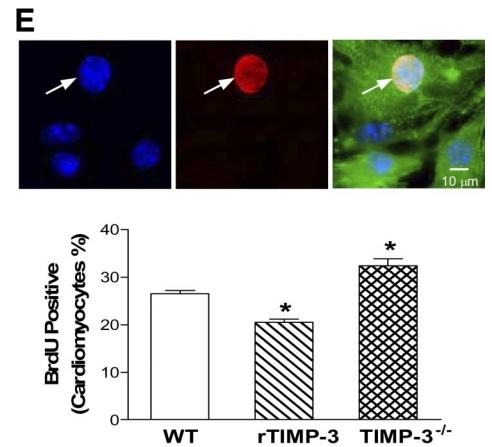
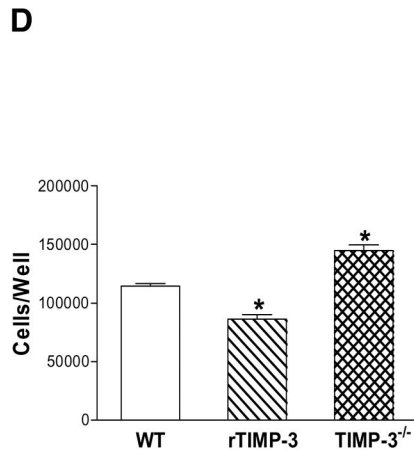
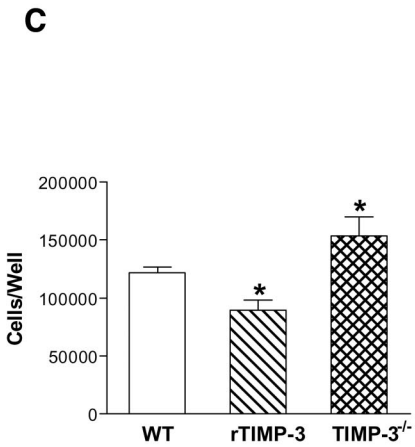
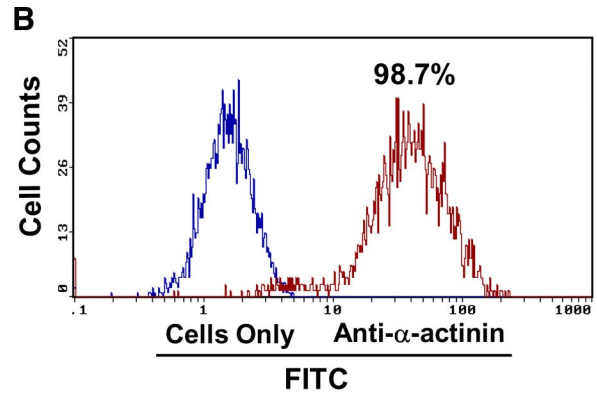
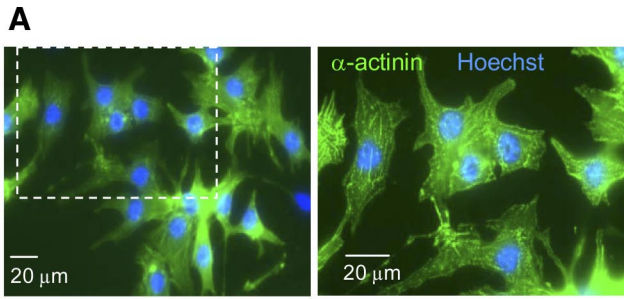
BrdU staining was also conducted to confirm cellular proliferation. Briefly, cells were grown on 1% gelatin-precoated coverglasses for 66 h, at which point the cells were treated with 10  $\mu$ M BrdU for 6 h. After BrdU incubation, cells were fixed in precooled 20% acetone-80% methanol. Subsequently, coverglasses were incubated with primary mouse monoclonal anti-BrdU (1:100 Sigma) and cardiac-specific  $\alpha$ -actinin (1:500, Sigma) antibodies. This was followed by incubations with respective secondary fluorescent antibodies. Hoechst 33342 was used to stain the nuclei. Data are presented as the percentage of BrdU-positive nuclei in cardiomyocytes.

*In vivo* neonatal cardiomyocyte proliferation was determined through nuclear Ki67 immunostaining on postnatal (*day 1*) heart sections similar to our previous reports (17, 21). Briefly, heart sections were incubated with anti-Ki67 (1:200, Lab Vision) and cardiac-specific  $\alpha$ -actinin (1:500, Sigma) antibodies. This was followed by incubations of respective secondary fluorescent antibodies. Hoechst 33342 was used to stain the nuclei. Data are presented as the percentage of Ki67-positive nuclei in cardiomyocytes.

*In vivo* adult cardiomyocyte proliferation was measured through BrdU staining. Adult mice were injected with BrdU (80 mg/kg ip) for 18 h. Hearts and small intestines (positive controls) were harvested. Frozen tissue sections (5  $\mu$ m) were incubated with a mouse anti-BrdU antibody (1:100, Sigma) followed by a biotinylated horse anti-mouse IgG (1:500, Vector Laboratories) in conjunction with an avidin-biotin-peroxidase amplification system (Vector Laboratories). The chromogen diaminobenzidine was used to detect BrdU incorporation with hematoxylin as a counterstain.

**Caspase-3 activity.** Caspase-3 activity was measured using the BIOMOL QuantiZyme Assay System (AK-700) as described previously (17, 21). Briefly, cell lysates containing 20  $\mu$ g of protein were incubated with the caspase-3 substrate Ac-DEVD-AMC in the presence or absence of the inhibitor Ac-DEVD-CHO at 37°C for 16 h. Fluorescence intensity was measured with the SpectraMax M5 microplate using excitation and emission wavelengths of 360 and 460 nm, respectively. Data are presented as the amount of AMC substrate cleaved per microgram protein.

Fig. 1. Cardiomyocyte purity and proliferation. *A*: cardiomyocytes were verified by cardiac-specific  $\alpha$ -actinin staining and examined under a fluorescence microscope at  $\times 400$ . The image at *right* is the boxed area examined at  $\times 630$ . *B*: cardiomyocyte purity was determined by flow cytometry using anti- $\alpha$ -actinin antibody. *C–E*: the number of cells per well was determined using a hemocytometer (*C*), verified using the CyQuant cell proliferation assay kit (*D*), and further confirmed through bromodeoxyuridine (BrdU) staining (*E*). A representative image of BrdU (arrows),  $\alpha$ -actinin (green) and Hoechst (blue) triple staining is shown in *E* (*top*). *F* and *G*: expression of the cell cycle promoter cyclin D1 (*F*) and cell cycle inhibitor p27 (*G*) was determined by real-time PCR analysis. *H*: general matrix metalloproteinase (MMP) activity was measured in media collected from cultured cardiomyocytes using the Sensolyte 520 Generic MMP assay kit. *C–H*: cultured neonatal wild-type (WT) cardiomyocytes were treated with recombinant mouse tissue inhibitor of metalloproteinase-3 (rTIMP-3; 1  $\mu$ g/ml). *I*: cardiomyocyte proliferation in postnatal *day 1* hearts was assessed through Ki67 staining. A representative image of Ki67 (arrows),  $\alpha$ -actinin (green), and Hoechst (blue) triple staining is shown (*top*). *J*: p27 mRNA in postnatal *day 1* hearts was analyzed by real-time PCR analysis. *K*: cardiomyocyte proliferation was also assessed in the adult hearts through BrdU staining, with the intestine as a positive control (+ve). Data are means  $\pm$  SE from 3–8 independent experiments. \**P* < 0.05 vs. WT control.



**MMP activity.** MMP activity was determined using the Sensolyte 520 Generic MMP Assay Kit (AnaSpec) as per manufacturer's instructions. Briefly, media from WT, TIMP-3<sup>-/-</sup>, and WT cells treated with rTIMP-3 (1 μg/ml) were collected 72 h postseeding, and 50 μl of these media were incubated with the FAM/QXL 520 fluorescence resonance energy transfer substrate for 1 h in a black 96-well plate at room temperature in the dark. Measurements were made using SpectraMax M5 microplate reader (excitation at 490 nm, emission at 520 nm). A standard curve was created using 5-FAM-Pro-Leu-OH to convert fluorescence values into amount of substrate cleaved. Values were normalized using the amount of protein lysed from WT, TIMP-3<sup>-/-</sup>, and rTIMP-3-treated wells and are expressed as pmoles substrate cleaved per milligram protein.

**Real-time RT-PCR.** Total RNA was extracted from cultured cardiomyocytes and neonatal heart tissues using TRIzol as previously described (28, 29). cDNA was synthesized using Moloney murine leukemia virus reverse transcriptase (Invitrogen, Burlington, ON, Canada). Real-time PCR was conducted using SYBR Green PCR Master Mix as per manufacturer's instructions (Eurogentec). 28S rRNA (housekeeping gene) was used as a loading control. The primer sequences were as follows: TIMP-3 upstream 5'-GAT GCC TTC TGC AAC TCC GA-3' and downstream 5'-CGG TCC AGA GAC ACT CAT TC-3'; p27 upstream 5'-TCG CAG AAC TTC GAA GAG

G-3' and downstream 5'-TGA CTC GCT TCT TCC ATA TCC-3' (19); EGFR upstream 5'-GAA CTG GGC TTA GGG AAC TGC-3' and downstream 5'-CATTGGGACAGCTTGG ATCAC-3'; cyclin D1 upstream 5'-CTG ACA CCA ATC TCC TCA ACG A-3' and downstream 5'-CTC ACA GAC CTC CAG CAT CCA-3'; 28S rRNA upstream 5'-TTG AAA ATC CGG GGG AGA G-3' and downstream 5'-ACA TTG TTC CAA CAT GCC AG-3'. Samples were amplified for 34 cycles using MJ Research Opticon Real-Time PCR machine. The levels of TIMP-3, p27, cyclin D1, and EGFR were compared with that of 28S rRNA, and the relative expression of these genes was determined in the same way as we previously described (17).

**Nuclear extraction.** Nuclear extractions were performed as previously described (39). Briefly, cardiomyocytes were lysed in *buffer A* (10 mM HEPES pH 7.9, 1 mM EDTA, 1 mM EGTA, 10 mM KCl, 1 mM DTT, 1 mM sodium vanadate, and 0.5% Nonidet P-40) containing proteinase inhibitors. The lysates were centrifuged (8,000 g, 15 min, 4°C), and the pellets were resuspended in *buffer B* (*buffer A* containing 20% glycerol and 0.4 M KCl). Following centrifugation (13,000 g, 15 min, 4°C), the supernatants were transferred to fresh tubes and used as the nuclear fraction.

**Electrophoretic mobility shift assay.** SP-1 DNA binding was analyzed by electrophoretic mobility shift assay (EMSA) as described previously (27). Nuclear extracts (10 μg) from WT cardiomyocytes

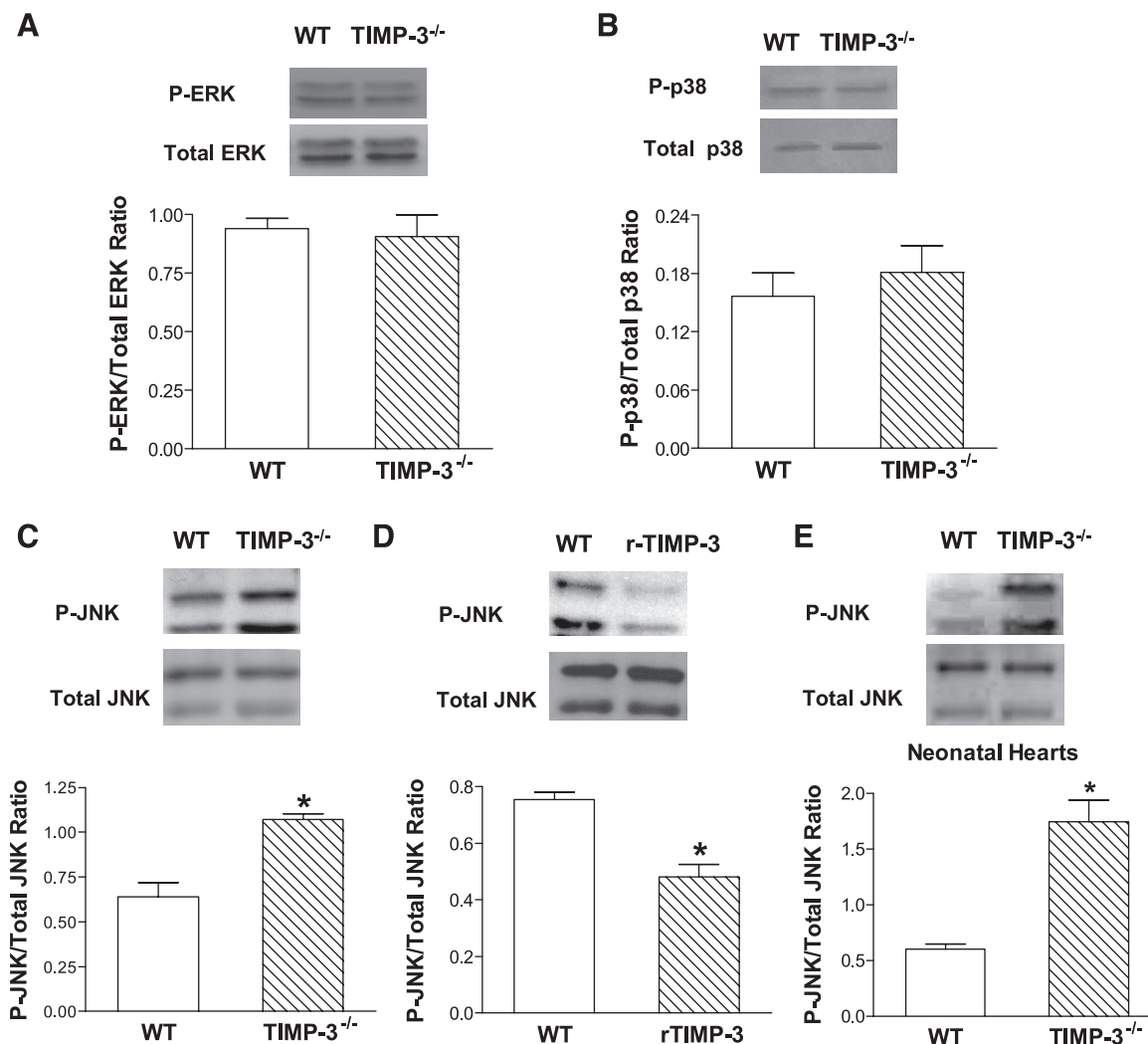


Fig. 2. Effect of TIMP-3 on MAPK phosphorylation in neonatal cardiomyocytes. Phosphorylation (P) of MAPKs in cultured neonatal WT and TIMP-3<sup>-/-</sup> cardiomyocytes was determined by Western blot analysis. A: ERK1/2. B: p38. C: JNK. D: effects of rTIMP-3 treatment (1 μg/ml). E: JNK phosphorylation in WT and TIMP-3<sup>-/-</sup> neonatal hearts. Data are means ± SE from 3–8 independent experiments. \**P* < 0.05 vs. WT control.

treated with DMSO (control) or MMA were incubated with the  $^{32}\text{P}$ -labeled SP-1 consensus oligonucleotide (SP-1: 5'-ATT CGA TCG GGG CGG GAG C-3'; Promega). Specificity was determined by the addition of an excess of unlabeled SP-1 oligonucleotide.

**Western blot analysis.** JNK, EGFR, and SP-1 protein levels were assessed by Western blotting. Briefly, cardiomyocyte lysates (from cells treated as described in *Cellular proliferation*) or neonatal heart tissue samples containing 30  $\mu\text{g}$  of protein or nuclear extracts were subjected to sodium dodecyl sulfate-polyacrylamide gel electrophoresis using 8–10% gels, followed by electrotransfer to polyvinylidene difluoride membranes. Blots were probed with antibodies against total and phosphorylated JNK, ERK, p38 (1:500; Cell Signaling Technology), total EGFR (1:300; Santa Cruz Biotechnology), phosphorylated EGFR (1:200; Cell Signaling Technology), phosphorylated-SP-1 (1:800; Santa Cruz Biotechnology),  $\beta$ -actin (1:2,000; Abcam), or cardiac-specific  $\alpha$ -actinin (1:2,000; Sigma) followed by incubation with horseradish peroxidase-conjugated secondary antibodies (1:2,000; Santa Cruz Biotechnology). Detection was performed using an enhanced chemiluminescence detection method. Signal intensity was quantified by densitometry. Levels of phospho-JNK, -ERK -p38, and -EGFR to their respective totals, as well as phospho-SP-1 to  $\beta$ -actin and total EGFR to  $\alpha$ -actinin are presented.

**Statistical analysis.** Data are presented as means  $\pm$  SE. Student's *t*-test and one- or two-way ANOVA followed by Newman-Keuls tests was performed.  $P < 0.05$  was considered statistically significant.

## RESULTS

**TIMP-3 inhibits mouse neonatal cardiomyocyte proliferation and MMP activity.** We recently showed that TIMP-3 regulates neonatal cardiomyocyte proliferation *in vitro* as well as *in vivo* (17). The aim of the current study was to delineate the mechanism by which TIMP-3 exerts its antiproliferative effects. To determine cardiomyocyte purity in our cell culture, a cardiomyocyte specific marker  $\alpha$ -actinin was used. Seventy-two hours postseeding, cardiomyocytes were stained positive

for cardiac  $\alpha$ -actinin (Fig. 1A). Purity of cardiomyocytes in our culture was 98.7% as determined by flow cytometric analysis (Fig. 1B). Cell proliferation was assessed by direct counting using a hemocytometer (Fig. 1C) and verified using the CyQuant Cell Proliferation Assay Kit (Fig. 1D) and through BrdU staining (Fig. 1E). *In vivo* cell proliferation was measured by counting the number of Ki67-positive cardiomyocytes in postnatal (*day 1*) mouse heart sections (Fig. 1I). In agreement with our previous studies (17), data showed that cell number was increased in the TIMP-3 $^{-/-}$  as compared with WT cardiomyocytes ( $P < 0.05$ ; Fig. 1, C–E), whereas treatment with rTIMP-3 significantly decreased cell number ( $P < 0.05$ ; Fig. 1, C–E). This is not due to decreased cell viability, because we recently showed that rTIMP-3 did not induce cardiomyocyte apoptosis (17). To investigate mechanisms by which TIMP-3 regulates cardiomyocyte proliferation, mRNA levels of cyclin D1 (a cell cycle promoter) and p27 (a cell cycle inhibitor) were determined by real-time RT-PCR (Fig. 1, F and G). Results showed that cyclin D1 expression was significantly increased (Fig. 1F) while p27 expression was significantly decreased (Fig. 1G) in TIMP-3 $^{-/-}$  cardiomyocytes, and the reverse was true in cardiomyocytes treated with rTIMP-3 as compared with WT ( $P < 0.05$ ). Furthermore, the number of Ki67-positive cardiomyocytes was significantly increased in TIMP-3 $^{-/-}$  heart tissues (Fig. 1I) while p27 expression was significantly reduced in TIMP-3 $^{-/-}$  hearts compared with WT (Fig. 1J). These data demonstrated that TIMP-3 promotes p27 expression and decreases cardiomyocyte proliferation. Because MMPs have a well-established role in promoting proliferation of various cell types including vascular smooth muscle cells (25), we measured general MMP activity in media collected from WT, rTIMP-3-treated, and TIMP-3 $^{-/-}$  cardiomyocytes. The results showed that MMP activity was significantly reduced in

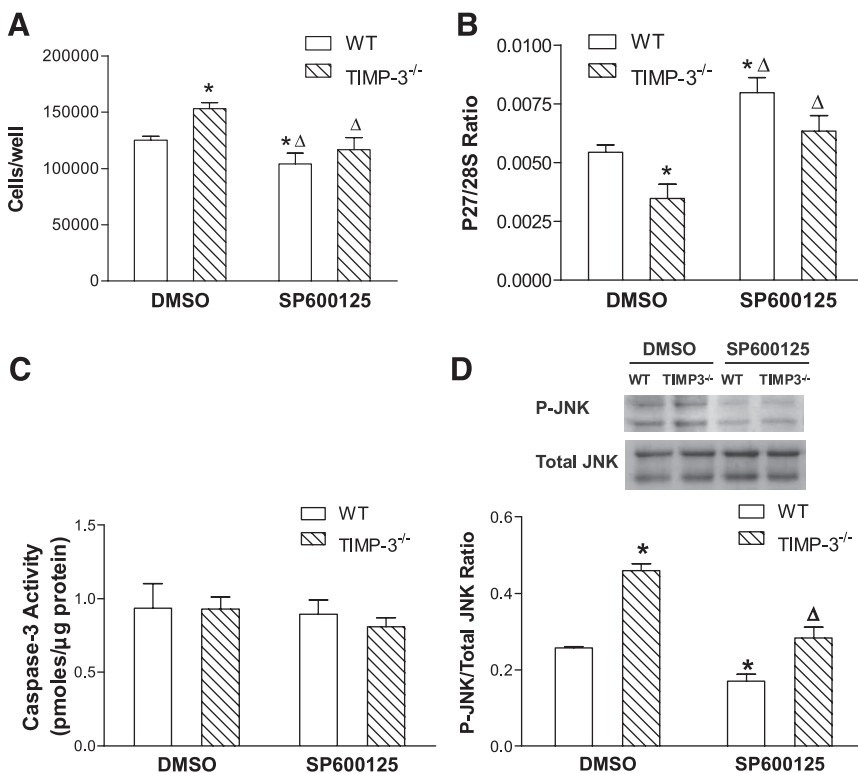


Fig. 3. Effect of JNK inhibition on cardiomyocyte proliferation and p27 expression. WT and TIMP-3 $^{-/-}$  neonatal cardiomyocytes were treated with the specific JNK inhibitor SP-600125 (10  $\mu\text{M}$ ) or dimethylsulfoxide (DMSO; control). Cell number per well was determined (A), and p27 expression was measured by real-time PCR analysis (B). Caspase-3 activity was measured (C), and the degree of JNK inhibition by SP-600126 was determined (D). Data are means  $\pm$  SE from 3–6 independent experiments. \* $P < 0.05$  vs. WT control,  $\Delta P < 0.05$  vs. TIMP-3 $^{-/-}$  control.

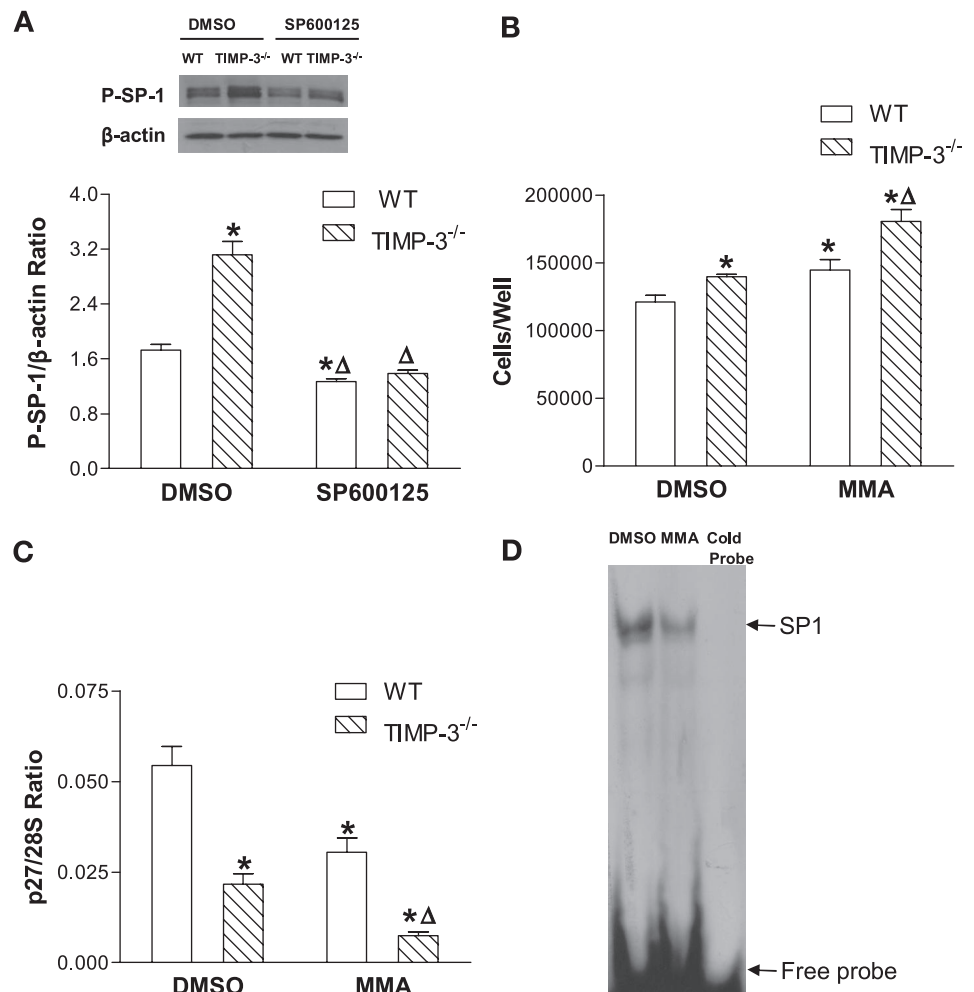
rTIMP-3-treated cardiomyocytes and significantly increased in TIMP-3<sup>-/-</sup> cells (Fig. 1H). To determine whether cardiomyocyte proliferation also occurred in adult mice, animals were treated with BrdU for 18 h, and BrdU incorporation was assessed using immunohistochemical staining, with the intestine as a positive control. Our data show that adult cardiomyocytes do not proliferate (Fig. 1K).

**TIMP-3 inhibits JNK phosphorylation.** To determine the mechanism by which TIMP-3 regulates p27 expression and, ultimately, proliferation, we investigated potential upstream targets of p27. Because MAPKs have previously been shown to promote proliferation of mammalian cells (40), we examined the effect of TIMP-3 on the phosphorylation of ERK1/2, p38, and JNK by Western blot analysis. The data showed that the levels of phosphorylated ERK1/2 (Fig. 2A) and p38 (Fig. 2B) did not change between WT and TIMP-3<sup>-/-</sup> cardiomyocytes. However, levels of phosphorylated JNK were significantly increased in TIMP-3<sup>-/-</sup> cardiomyocytes ( $P < 0.05$ ; Fig. 2C) and decreased in rTIMP-3-treated cells ( $P < 0.05$ ; Fig. 2D) compared with WT controls. To confirm this finding in vivo, the levels of phosphorylated JNK were measured in WT and TIMP-3<sup>-/-</sup> heart tissues. The data showed that JNK phosphorylation was significantly increased in TIMP-3<sup>-/-</sup> compared with WT hearts ( $P < 0.05$ ; Fig. 2E).

**JNK increases cardiomyocyte proliferation and decreases p27 expression.** The effect of JNK on neonatal cardiomyocyte proliferation and p27 expression was examined by treating WT and TIMP-3<sup>-/-</sup> cardiomyocytes with the specific JNK inhibitor SP-600125. The data showed that inhibition of JNK leads to a significant decrease in cardiomyocyte proliferation ( $P < 0.05$ ; Fig. 3A) and a concomitant increase in p27 expression in WT and TIMP-3<sup>-/-</sup> cardiomyocytes ( $P < 0.05$ ; Fig. 3B). To verify that the decrease in proliferation with SP-600125 treatment is not due to an increase in apoptosis, caspase-3 activity was measured in WT and TIMP-3<sup>-/-</sup> cardiomyocytes treated with the specific JNK inhibitor SP-600125. Our data showed that caspase-3 activity did not change with SP-600125 treatment ( $P =$  not significant; Fig. 3C). Furthermore, JNK phosphorylation was significantly decreased by SP-600125 treatment ( $P < 0.05$ ; Fig. 3D).

**JNK increases SP-1 phosphorylation and cardiomyocyte proliferation and inhibits p27 expression.** To determine whether JNK regulates p27 expression through phosphorylation of SP-1, WT and TIMP-3<sup>-/-</sup> cardiomyocytes were cultured and treated with the JNK inhibitor SP-600125. Nuclear extraction was performed, and the extracts were subjected to Western blot analysis. The data showed that phosphorylated levels of SP-1 were significantly increased in TIMP-3<sup>-/-</sup>

Fig. 4. Effect of JNK inhibition on SP-1 phosphorylation, cardiomyocyte proliferation, and p27 expression. **A:** WT and TIMP-3<sup>-/-</sup> neonatal cardiomyocytes were treated with the JNK inhibitor SP-600125 (10  $\mu$ M). Nuclear extracts were isolated, and the levels of phosphorylated SP-1/ $\beta$ -actin were determined through Western blot analysis. **B** and **C:** WT and TIMP-3<sup>-/-</sup> neonatal cardiomyocytes were treated with the SP-1 inhibitor mithramycin (MMA, 10 nM) or DMSO (control). Cell number per well was determined (**B**), and p27 expression was measured by real-time PCR analysis (**C**). **D:** inhibition of SP-1 binding activity by MMA was verified by EMSA. Data are means  $\pm$  SE from 3–5 independent experiments. \* $P < 0.05$  vs. WT control,  $\Delta P < 0.05$  vs. TIMP-3<sup>-/-</sup> control.



cardiomyocytes ( $P < 0.05$ ; Fig. 4A). Furthermore, treatment with SP-600125 significantly decreased phosphorylated SP-1 levels in both WT and TIMP-3<sup>-/-</sup> cardiomyocytes ( $P < 0.05$ ; Fig. 4A), suggesting that JNK increases SP-1 phosphorylation.

The p27 promoter has several SP-1 binding sites, and p27 expression is regulated by SP-1 binding to the p27 promoter in various cell types, including tumor cells (15) and vascular smooth muscle cells (2). To determine whether SP-1 regulates p27 expression in neonatal cardiomyocytes, WT and TIMP-3<sup>-/-</sup> cardiomyocytes were treated with MMA, a selective inhibitor of SP-1 DNA binding activity (3). Our results showed that inhibition of SP-1 significantly increased cardiomyocyte proliferation ( $P < 0.05$ ; Fig. 4B) and significantly decreased p27 expression ( $P < 0.05$ ; Fig. 4C). To verify that MMA inhibits SP-1 binding in cardiomyocytes, cells were treated with DMSO or MMA as above, and an EMSA was performed. The results showed that, indeed, MMA inhibited SP-1 DNA binding activity (Fig. 4D).

**EGFR increases neonatal cardiomyocyte proliferation and JNK phosphorylation.** EGFR has previously been shown to promote proliferation of various cell types such as cancer cells and to activate various MAPKs (4, 10, 33). To determine the pathway upstream of JNK, we examined whether EGFR was involved. To that end, WT and TIMP-3<sup>-/-</sup> cardiomyocytes were treated with a specific EGFR inhibitor, PD-168393. Cell proliferation was determined by cell counts, and the effect of EGFR inhibition on JNK phosphorylation was examined by Western blot analysis. Inhibition of EGFR significantly reduced cardiomyocyte proliferation ( $P < 0.05$ ; Fig. 5A) and JNK phosphorylation ( $P < 0.05$ ; Fig. 5B). The results suggest that activation of EGFR increases cardiomyocyte proliferation and JNK activation.

**TIMP-3 inhibits EGFR expression in neonatal cardiomyocytes.** Because our data demonstrated that both TIMP-3 and EGFR regulated proliferation and JNK activation, we wanted to determine whether TIMP-3 was acting upstream of EGFR. We examined EGFR mRNA expression in WT and TIMP-3<sup>-/-</sup> cardiomyocytes treated with and without rTIMP-3. Real-time PCR analysis showed that EGFR mRNA expression was significantly increased in TIMP-3<sup>-/-</sup> cardiomyocytes ( $P < 0.05$ ; Fig. 6A) and was significantly decreased by rTIMP-3 ( $P < 0.05$ ; Fig. 6B). Furthermore, EGFR mRNA expression was significantly elevated in TIMP-3<sup>-/-</sup> hearts ( $P < 0.05$ ; Fig. 6C). Our data also showed that EGFR protein expression was increased in TIMP-3<sup>-/-</sup> cardiomyocytes ( $P < 0.05$ ; Fig. 6D) and decreased in cardiomyocytes treated with rTIMP-3 ( $P < 0.05$ ; Fig. 6E). To determine whether TIMP-3 regulated EGFR expression in vivo, EGFR expression was measured in WT and TIMP-3<sup>-/-</sup> neonatal hearts. Our data demonstrated a significant increase in EGFR protein expression in TIMP-3<sup>-/-</sup> heart tissues compared with WT ( $P < 0.05$ ; Fig. 6F). Taken together, our results suggest that TIMP-3 decreases EGFR expression in cardiomyocytes in vitro and in vivo. To determine whether the TIMP-3-mediated change in EGFR expression led to a change in EGFR activation, we measured the levels of phosphorylated EGFR in WT, TIMP-3<sup>-/-</sup>, and rTIMP-3-treated cells. Our data showed that levels of phosphorylated EGFR (P-EGFR) were significantly elevated in TIMP-3<sup>-/-</sup> cells ( $P < 0.05$ ; Fig. 6G) and significantly reduced in rTIMP-3-treated cardiomyocytes ( $P < 0.05$ ; Fig. 6H).

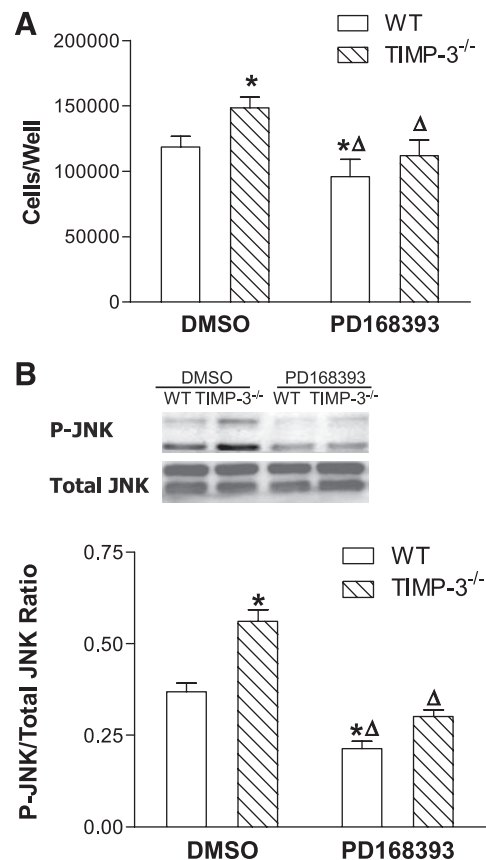


Fig. 5. Effect of epidermal growth factor (EGF) receptor (EGFR) inhibition on cardiomyocyte proliferation and JNK phosphorylation. WT and TIMP-3<sup>-/-</sup> neonatal cardiomyocytes were treated with the selective EGFR inhibitor PD-168393 (10  $\mu$ M). Cell proliferation was determined by direct cell counts (A), and the levels of phosphorylated JNK/total JNK were measured by Western blot analysis (B). Data are means  $\pm$  SE from 4–5 independent experiments. \* $P < 0.05$  vs. WT control,  $\Delta P < 0.05$  vs. TIMP-3<sup>-/-</sup> control.

**TIMP-3 regulates the EGFR/SP-1 proliferation pathway through EGF.** All of the EGFR ligands are synthesized as membrane-tethered precursors and are shed by metalloproteinases (32), which are inhibited by TIMP-3 (5). Since EGF is an abundant EGFR ligand and has a well-established role in fetal cardiomyocyte proliferation (16), we wanted to determine the role of EGF in neonatal cardiomyocyte proliferation, SP-1 phosphorylation, and EGFR expression. WT and TIMP-3<sup>-/-</sup> cardiomyocytes were treated with the EGF-neutralizing antibody. Our data showed that EGF neutralization significantly decreased cell proliferation and SP-1 phosphorylation in WT and TIMP-3<sup>-/-</sup> cardiomyocytes ( $P < 0.05$ ; Fig. 7, A and C), suggesting that EGF promotes neonatal cardiomyocyte proliferation and SP-1 phosphorylation. Furthermore, treatment with the EGF-neutralizing antibody significantly decreased EGFR expression in WT and TIMP-3<sup>-/-</sup> cardiomyocytes ( $P < 0.05$ ; Fig. 7D), suggesting that EGFR regulates its own expression through ligand binding. Interestingly, EGF neutralization decreased SP-1 phosphorylation by 40% vs. 89% and decreased EGFR expression by 27% vs. 91% in WT and TIMP-3<sup>-/-</sup> cardiomyocytes, respectively (Fig. 7, C and D;  $P < 0.05$ ). The results suggest an increased EGFR/SP1 signaling in TIMP-3<sup>-/-</sup> cardiomyocytes and support an important role for TIMP-3 in inhibiting EGF/EGFR/SP-1 signaling. To further

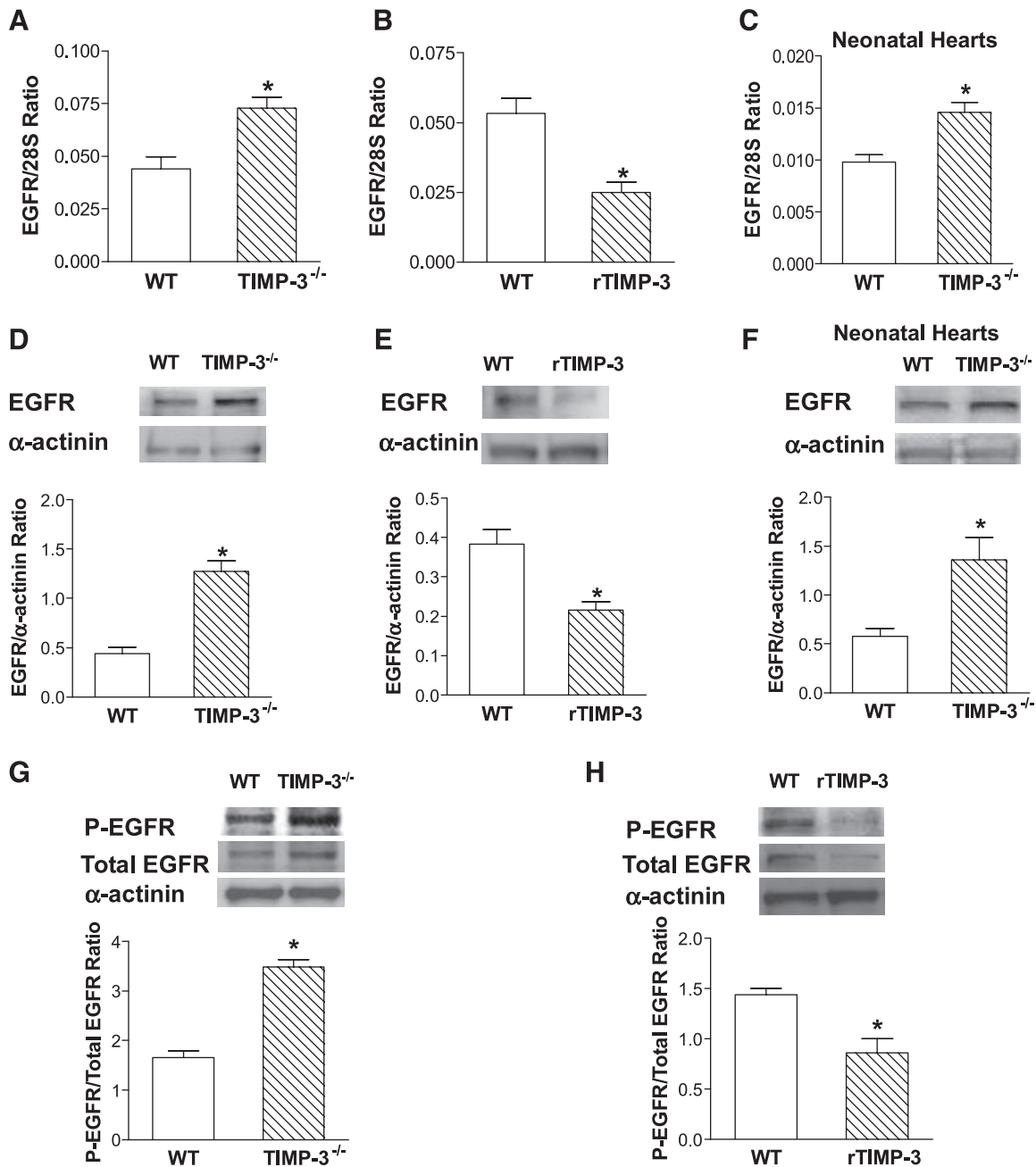


Fig. 6. Effect of TIMP-3 on EGFR expression/phosphorylation in neonatal cardiomyocytes. *A*, *D*, and *G*: EGFR mRNA (*A*), protein expression (*D*), and phosphorylation (*G*) in cultured WT and TIMP-3<sup>-/-</sup> cardiomyocytes. *B*, *E*, and *H*: effects of recombinant TIMP-3 (1 µg/ml) treatment on EGFR mRNA (*B*), protein expression (*E*), and phosphorylation (*H*) in WT cardiomyocytes. *C* and *F*: EGFR mRNA (*C*) and protein (*F*) levels in neonatal hearts. EGFR protein expression, phosphorylation, and mRNA levels were analyzed by Western blot and real-time PCR analysis, respectively. Cardiac-specific α-actinin and 28S were used as loading controls. Data are means ± SE from 3–5 independent experiments. \**P* < 0.05 vs. WT control.

verify the effect of EGF on cardiomyocyte proliferation and determine its effect on EGFR phosphorylation, WT and TIMP-3<sup>-/-</sup> cardiomyocytes were treated with rEGF. Our data showed that treatment with rEGF resulted in a significant increase in proliferation and P-EGFR phosphorylation in WT cardiomyocytes (*P* < 0.05; Fig. 7, *B* and *E*). However, rEGF had minimal effect on proliferation and P-EGFR levels in TIMP-3<sup>-/-</sup> cardiomyocytes (*P* < 0.05; Fig. 7, *B* and *E*), probably due to the already high proliferation levels in these cells. Our results support the notion that EGF is probably a

major ligand for EGFR activation and cell proliferation in cardiomyocytes.

#### DISCUSSION

We have recently demonstrated that TIMP-3 decreases neonatal cardiomyocyte proliferation (17). The aim of the present study was to delineate a signaling pathway by which TIMP-3 achieves this effect. We showed that rTIMP-3 decreased MMP activity and EGFR expression, leading to decreased phosphor-

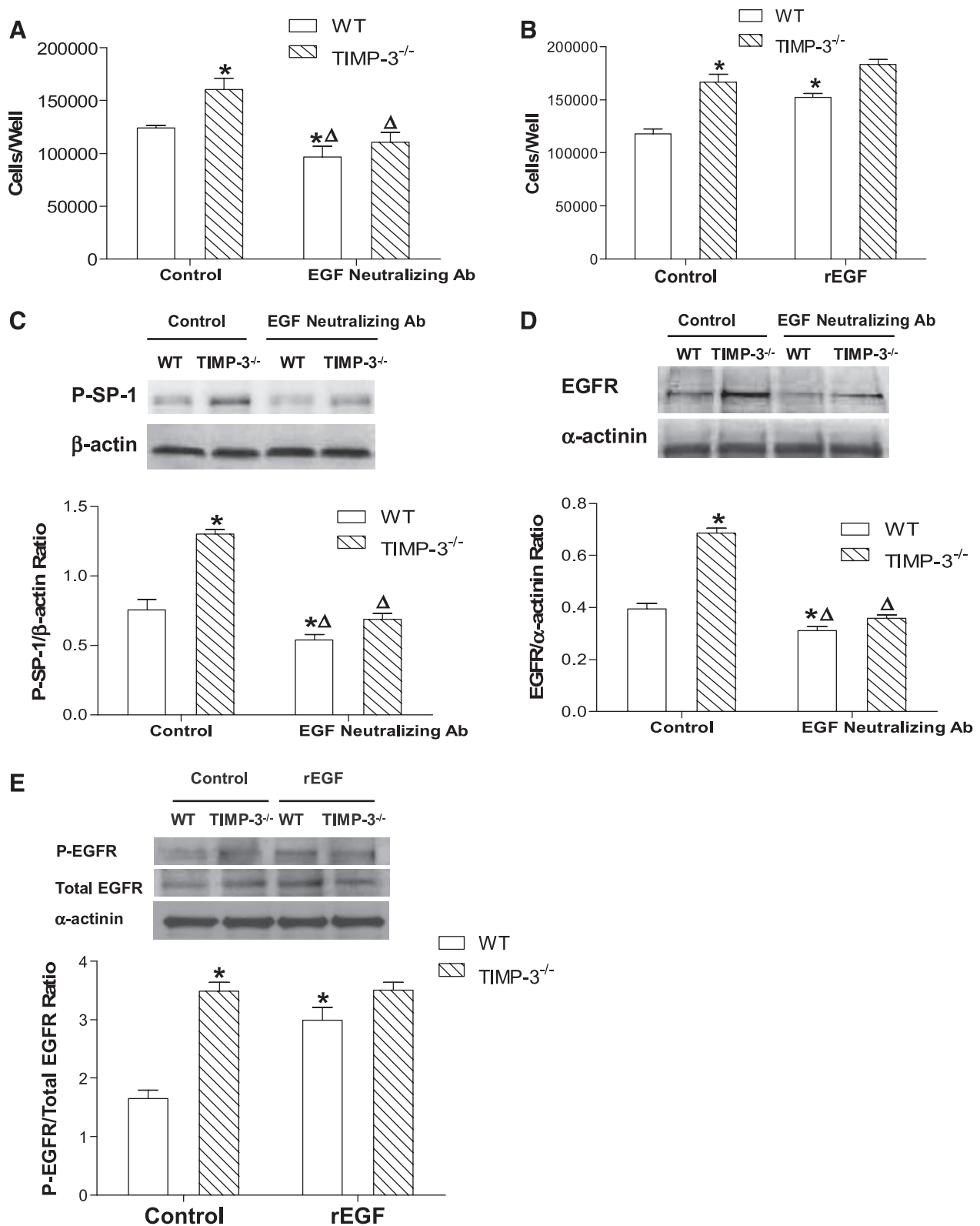


Fig. 7. Effect of EGF on neonatal cardiomyocyte proliferation, SP-1 phosphorylation, and EGFR expression/phosphorylation. Cultured WT and TIMP-3<sup>-/-</sup> cardiomyocytes were treated with 20  $\mu$ g/ml EGF neutralizing antibody (Ab) or 100 ng/ml recombinant EGF. *A* and *B*: cell proliferation was assessed by direct cell counts. *C–E*: levels of phosphorylated SP-1/ $\beta$ -actin (*C*) and of EGFR protein expression (*D*) and phosphorylation (*E*) were determined by Western blot analysis. Data are means  $\pm$  SE from 3–4 independent experiments. \**P* < 0.05 vs. WT control,  $\Delta$ *P* < 0.05 vs. TIMP-3<sup>-/-</sup> control.

ylation of JNK and SP-1. Decreased phosphorylation of SP-1 upregulated cell cycle inhibitor p27 expression, resulting in inhibition of cardiomyocyte proliferation. Our data suggest that TIMP-3 regulates cardiomyocyte proliferation via the EGFR/JNK/SP-1/p27 signaling pathway (Fig. 8).

Cell proliferation is regulated by the balance between cyclin-dependent kinases (CDKs) and CDK inhibitors such as p27. In neonatal cardiomyocytes, p27 is a key inhibitor of cell proliferation (6) and cyclin D1 is important for cell cycle progression (36). To delineate the pathway through which TIMP-3 inhibits neonatal cardiomyocyte proliferation, the effect of TIMP-3 on cyclin D1 and p27 expression was investigated. Our data showed that cyclin D1 was increased in TIMP-3<sup>-/-</sup> cardiomyocytes and decreased in rTIMP-3-treated cells as compared with WT. Consistent with these results, p27 expression was decreased in the TIMP-3<sup>-/-</sup> cardiomyocytes and neonatal hearts as compared with WT. This decrease in p27 expression resulted in an increase in cardiomyocyte proliferation both in vitro and in vivo. Furthermore, treatment of cardiomyocytes with rTIMP-3 resulted in a significant increase in p27 expression, which led to a significant decrease in cardiomyocyte proliferation. Our data suggest that TIMP-3 inhibits cardiomyocyte proliferation via modulation of cell cycle regulators.

MAPK signaling is implicated in the promotion of cell proliferation (33). For example, activation of JNK, ERK, and p38 contributes to proliferation and cardiomyocyte differentiation of P19 cells (12). To study the role of MAPK in cardiomyocyte proliferation, we measured phosphorylation of JNK, ERK1/2, and p38. Data showed that phosphorylation of ERK1/2 and p38 was not significantly altered; however, JNK phosphorylation was increased in TIMP-3<sup>-/-</sup> cardiomyocytes and neonatal hearts compared with those of WT. Treatment with rTIMP-3 significantly decreased JNK phosphorylation. Furthermore, inhibition of JNK increased p27 expression and concomitantly decreased cardiomyocyte proliferation. Our re-

sults demonstrated that TIMP-3 inhibits JNK activation in cardiomyocytes and that inhibition of JNK phosphorylation decreases cardiomyocyte proliferation.

The transcriptional factor SP-1 regulates p27 expression. The promoter region of p27 has several SP-1 binding sites, and binding of unphosphorylated SP-1 to the p27 promoter increases p27 expression and inhibits proliferation in cancer cells (15). In the present study, we examined the effect of SP-1 on p27 expression and neonatal cardiomyocyte proliferation. Our data demonstrated that inhibition of SP-1 activity by MMA decreased p27 expression and increased cardiomyocyte proliferation. Furthermore, increased JNK activation in TIMP-3<sup>-/-</sup> cardiomyocytes was associated with increased SP-1 phosphorylation and decreased p27 expression. Moreover, JNK inhibition by SP-600125 decreased SP-1 phosphorylation, increased p27 expression, and decreased cardiomyocyte proliferation in both WT and TIMP-3<sup>-/-</sup> cardiomyocytes. Taken together, these data suggest that SP-1 is downstream of JNK and that phosphorylation of SP-1 by JNK decreases p27 expression and increases cardiomyocyte proliferation in TIMP-3<sup>-/-</sup> cardiomyocytes.

It is well established that EGF/EGFR signaling promotes cell proliferation including fetal cardiomyocyte proliferation (16). Activation of EGFR increases phosphorylation of MAPKs including JNK in neonatal cardiomyocytes (31). However, the role of TIMP-3 in EGF/EGFR signaling has not been demonstrated in cardiomyocytes. EGF is synthesized as an integral membrane protein that can be proteolytically cleaved and shed from cells. Activation of metalloproteinase is crucial for EGF shedding and thus EGFR activation (32). Since TIMP-3 is a potent inhibitor of metalloproteinases, we investigated the effects of TIMP-3 on MMP activity and EGF/EGFR signaling in the present study. Our data showed that MMP activity was increased in TIMP-3<sup>-/-</sup> neonatal cardiomyocytes and decreased with rTIMP-3 treatment. Furthermore, EGFR expression was significantly increased in TIMP-3<sup>-/-</sup> cardiomyocytes in vitro and TIMP-3<sup>-/-</sup> hearts in vivo. Moreover, treatment with rTIMP-3 resulted in a significant decrease in EGFR expression and EGFR phosphorylation in cardiomyocytes. Additionally, the phosphorylation of JNK and SP-1 was increased in TIMP-3<sup>-/-</sup> neonatal cardiomyocytes, which was also inhibited by rTIMP-3 and a JNK inhibitor, respectively. These results demonstrated an inhibitory role for TIMP-3 in EGFR/JNK/SP-1 signaling in cardiomyocytes. To determine whether EGF is the ligand responsible for EGFR signaling and cardiomyocyte proliferation, cardiomyocytes were treated with an EGF-neutralizing antibody or an EGF recombinant protein. EGF neutralization significantly decreased EGFR expression, SP-1 phosphorylation, and proliferation in WT and TIMP-3<sup>-/-</sup> cardiomyocytes. Interestingly, treatment with rEGF resulted in a significant increase in EGFR phosphorylation and proliferation in WT cardiomyocytes but not in TIMP-3<sup>-/-</sup> cells, suggesting that the EGF/EGFR pathway is near maximal activation in the knockout cells such that addition of EGF does not lead to further activation of the pathway. The results are consistent with the notion that EGFR ligands promote EGFR expression through a positive feedback mechanism (8, 9) and that EGF/EGFR signaling contributes to increased proliferation in TIMP-3<sup>-/-</sup> cardiomyocytes.

In summary, TIMP-3 inhibits neonatal cardiomyocyte proliferation in vitro as well as in vivo. These effects of TIMP-3

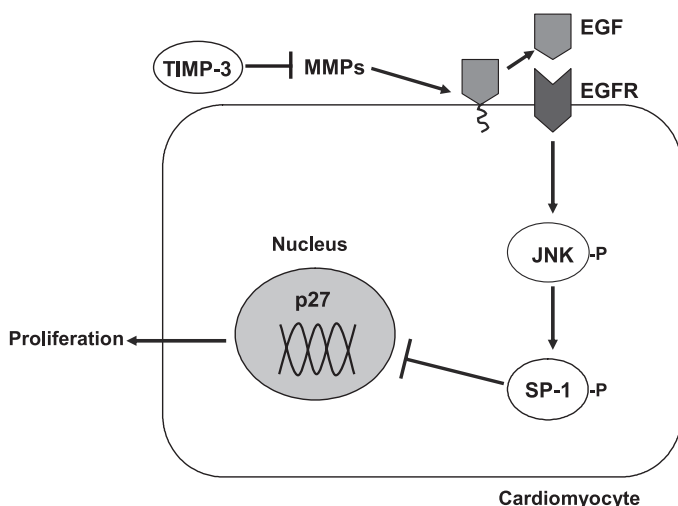


Fig. 8. Proposed signaling pathway by which TIMP-3 inhibits neonatal cardiomyocyte proliferation. TIMP-3 is a potent inhibitor of MMPs. Metalloproteinases are known to shed many membrane proteins including EGF, a ligand of the EGFR. EGF activates EGFR, a receptor tyrosine kinase, which then activates mitogen-activated protein kinases including JNK. Activated JNK phosphorylates a variety of transcription factors including SP-1. Phosphorylated SP-1 reduces p27 expression, resulting in increased cardiomyocyte proliferation.

are mediated through the inhibition of MMP activity and downregulation of EGF/EGFR signaling, leading to reductions in JNK and SP-1 phosphorylation, and upregulation of p27 expression (Fig. 8).

#### GRANTS

This study was supported by operating grants from Canadian Institutes of Health Research (CIHR, MOP-64395) and Heart and Stroke Foundation of Ontario (HSFO, T-6040) awarded to Q. Feng. L. Hammoud is supported by a Heart and Stroke Foundation of Canada Doctoral Research Award. Q. Feng is a HSFO Career Investigator.

#### REFERENCES

- Amour A, Slocombe PM, Webster A, Butler M, Knight CG, Smith BJ, Stephens PE, Shelley C, Hutton M, Knauper V, Docherty AJ, Murphy G. TNF-alpha converting enzyme (TACE) is inhibited by TIMP-3. *FEBS Lett* 435: 39–44, 1998.
- Andres V, Urena J, Poch E, Chen D, Goukassian D. Role of Sp1 in the induction of p27 gene expression in vascular smooth muscle cells in vitro and after balloon angioplasty. *Arterioscler Thromb Vasc Biol* 21: 342–347, 2001.
- Blondet A, Gout J, Durand P, Begoot M, Naville D. Expression of the human melanocortin-4 receptor gene is controlled by several members of the Sp transcription factor family. *J Mol Endocrinol* 34: 317–329, 2005.
- Bost F, McKay R, Dean N, Mercola D. The JUN kinase/stress-activated protein kinase pathway is required for epidermal growth factor stimulation of growth of human A549 lung carcinoma cells. *J Biol Chem* 272: 33422–33429, 1997.
- Brew K, Dinakarpanian D, Nagase H. Tissue inhibitors of metalloproteinases: evolution, structure and function. *Biochim Biophys Acta* 1477: 267–283, 2000.
- Brooks G, Poolman RA, Li JM. Arresting developments in the cardiac myocyte cell cycle: role of cyclin-dependent kinase inhibitors. *Cardiovasc Res* 39: 301–311, 1998.
- Burger D, Lei M, Geoghegan-Morphet N, Lu X, Xenocostas A, Feng Q. Erythropoietin protects cardiomyocytes from apoptosis via up-regulation of endothelial nitric oxide synthase. *Cardiovasc Res* 72: 51–59, 2006.
- Citri A, Yarden Y. EGF-ERBB signalling: towards the systems level. *Nat Rev Mol Cell Biol* 7: 505–516, 2006.
- Clark AJ, Ishii S, Richert N, Merlino GT, Pastan I. Epidermal growth factor regulates the expression of its own receptor. *Proc Natl Acad Sci USA* 82: 8374–8378, 1985.
- Coso OA, Chiariello M, Yu JC, Teramoto H, Crespo P, Xu N, Miki T, Gutkind JS. The small GTP-binding proteins Rac1 and Cdc42 regulate the activity of the JNK/SAPK signaling pathway. *Cell* 81: 1137–1146, 1995.
- Deshmukh HS, Case LM, Wesselkamper SC, Borchers MT, Martin LD, Shertzer HG, Nadel JA, Leikauf GD. Metalloproteinases mediate mucin 5AC expression by epidermal growth factor receptor activation. *Am J Respir Crit Care Med* 171: 305–314, 2005.
- Eriksson M, Leppa S. Mitogen-activated protein kinases and activator protein 1 are required for proliferation and cardiomyocyte differentiation of P19 embryonal carcinoma cells. *J Biol Chem* 277: 15992–16001, 2002.
- Fedak PW, Altamentova SM, Weisel RD, Nili N, Ohno N, Verma S, Lee TY, Kiani C, Mickle DA, Strauss BH, Li RK. Matrix remodeling in experimental and human heart failure: a possible regulatory role for TIMP-3. *Am J Physiol Heart Circ Physiol* 284: H626–H634, 2003.
- Fedak PW, Smookler DS, Kassiri Z, Ohno N, Leco KJ, Verma S, Mickle DA, Watson KL, Hojilla CV, Cruz W, Weisel RD, Li RK, Khokha R. TIMP-3 deficiency leads to dilated cardiomyopathy. *Circulation* 110: 2401–2409, 2004.
- Fischer C, Sanchez-Ruderis H, Welzel M, Wiedenmann B, Sakai T, Andre S, Gabius HJ, Khachigian L, Detjen KM, Rosewicz S. Galectin-1 interacts with the  $\alpha_5\beta_1$  fibronectin receptor to restrict carcinoma cell growth via induction of p21 and p27. *J Biol Chem* 280: 37266–37277, 2005.
- Goldman B, Mach A, Wurzel J. Epidermal growth factor promotes a cardiomyoblastic phenotype in human fetal cardiac myocytes. *Exp Cell Res* 228: 237–245, 1996.
- Hammoud L, Xiang F, Lu X, Brunner F, Leco K, Feng Q. Endothelial nitric oxide synthase promotes neonatal cardiomyocyte proliferation by inhibiting tissue inhibitor of metalloproteinase-3 expression. *Cardiovasc Res* 75: 359–368, 2007.
- Harris RC, Chung E, Coffey RJ. EGF receptor ligands. *Exp Cell Res* 284: 2–13, 2003.
- Kwon YH, Jovanovic A, Serfas MS, Tyner AL. The Cdk inhibitor p21 is required for necrosis, but it inhibits apoptosis following toxin-induced liver injury. *J Biol Chem* 278: 30348–30355, 2003.
- Leco KJ, Waterhouse P, Sanchez OH, Gowing KL, Poole AR, Wakeham A, Mak TW, Khokha R. Spontaneous air space enlargement in the lungs of mice lacking tissue inhibitor of metalloproteinases-3 (TIMP-3). *J Clin Invest* 108: 817–829, 2001.
- Lepic E, Burger D, Lu X, Song W, Feng Q. Lack of endothelial nitric oxide synthase decreases cardiomyocyte proliferation and delays cardiac maturation. *Am J Physiol Cell Physiol* 291: C1240–C1246, 2006.
- Li F, Wang X, Capasso JM, Gerdes AM. Rapid transition of cardiac myocytes from hyperplasia to hypertrophy during postnatal development. *J Mol Cell Cardiol* 28: 1737–1746, 1996.
- Liu YT, Song L, Templeton DM. Heparin suppresses lipid raft-mediated signaling and ligand-independent EGF receptor activation. *J Cell Physiol* 211: 205–212, 2007.
- MacLellan WR, Schneider MD. Genetic dissection of cardiac growth control pathways. *Annu Rev Physiol* 62: 289–319, 2000.
- Newby AC. Matrix metalloproteinases regulate migration, proliferation, and death of vascular smooth muscle cells by degrading matrix and non-matrix substrates. *Cardiovasc Res* 69: 614–624, 2006.
- Pasumarthi KB, Field LJ. Cardiomyocyte cell cycle regulation. *Circ Res* 90: 1044–1054, 2002.
- Peng T, Lu X, Feng Q. NADH oxidase signaling induces cyclooxygenase-2 expression during lipopolysaccharide stimulation in cardiomyocytes. *FASEB J* 19: 293–295, 2005.
- Peng T, Lu X, Feng Q. Pivotal role of gp91phox-containing NADH oxidase in lipopolysaccharide-induced tumor necrosis factor- $\alpha$  expression and myocardial depression. *Circulation* 111: 1637–1644, 2005.
- Peng T, Lu X, Lei M, Feng Q. Endothelial nitric-oxide synthase enhances lipopolysaccharide-stimulated tumor necrosis factor- $\alpha$  expression via cAMP-mediated p38 MAPK pathway in cardiomyocytes. *J Biol Chem* 278: 8099–8105, 2003.
- Poolman RA, Li JM, Durand B, Brooks G. Altered expression of cell cycle proteins and prolonged duration of cardiac myocyte hyperplasia in p27KIP1 knockout mice. *Circ Res* 85: 117–127, 1999.
- Purdom S, Chen QM. Epidermal growth factor receptor-dependent and -independent pathways in hydrogen peroxide-induced mitogen-activated protein kinase activation in cardiomyocytes and heart fibroblasts. *J Pharmacol Exp Ther* 312: 1179–1186, 2005.
- Sahin U, Weskamp G, Kelly K, Zhou HM, Higashiyama S, Peschon J, Hartmann D, Saftig P, Blobel CP. Distinct roles for ADAM10 and ADAM17 in ectodomain shedding of six EGFR ligands. *J Cell Biol* 164: 769–779, 2004.
- Schlessinger J. Cell signaling by receptor tyrosine kinases. *Cell* 103: 211–225, 2000.
- Song W, Lu X, Feng Q. Tumor necrosis factor- $\alpha$  induces apoptosis via inducible nitric oxide synthase in neonatal mouse cardiomyocytes. *Cardiovasc Res* 45: 595–602, 2000.
- Spinale FG. Matrix metalloproteinases: regulation and dysregulation in the failing heart. *Circ Res* 90: 520–530, 2002.
- Tamamori-Adachi M, Ito H, Sumrejkanchanakij P, Adachi S, Hiroe M, Shimizu M, Kawauchi J, Sunamori M, Marumo F, Kitajima S, Ikeda MA. Critical role of cyclin D1 nuclear import in cardiomyocyte proliferation. *Circ Res* 92: e12–e19, 2003.
- Visse R, Nagase H. Matrix metalloproteinases and tissue inhibitors of metalloproteinases: structure, function, and biochemistry. *Circ Res* 92: 827–839, 2003.
- Woessner JF Jr. That impish TIMP: the tissue inhibitor of metalloproteinases-3. *J Clin Invest* 108: 799–800, 2001.
- Zeidan A, Javadov S, Chakrabarti S, Karmazyn M. Leptin-induced cardiomyocyte hypertrophy involves selective caveolae and RhoA/ROCK-dependent p38 MAPK translocation to nuclei. *Cardiovasc Res* 77: 64–72, 2008.
- Zhang W, Liu HT. MAPK signal pathways in the regulation of cell proliferation in mammalian cells. *Cell Res* 12: 9–18, 2002.
- Zhao YY, Sawyer DR, Baliga RR, Opel DJ, Han X, Marchionni MA, Kelly RA. Neuregulins promote survival and growth of cardiac myocytes. Persistence of ErbB2 and ErbB4 expression in neonatal and adult ventricular myocytes. *J Biol Chem* 273: 10261–10269, 1998.